

## AERODYNAMIC PERFORMANCE OF THE REVERSIBLE AXIAL FAN FOR HIGH AIR TEMPERATURES

by

**Živan T. SPASIĆ\***, **Veljko S. BEGOVIĆ**, **Saša M. MILANOVIĆ**,  
**and Miloš M. JOVANOVIĆ**

Faculty of Mechanical Engineering, University of Niš, Niš, Serbia

Original scientific paper

<https://doi.org/10.2298/TSCI230405135S>

*The paper presents the aerodynamic performance of an axial reversible fan for high air temperatures, obtained by applying the similarity theory and numerical flow simulations. This analysis was performed for the possibility of installing the existing structure of an impeller of a reversible fan in a jet fan for the longitudinal ventilation of a tunnel. The direction of forced flow in tunnels changes, and it is always towards low atmospheric pressure, i.e. in the direction of natural air-flow. These fans often work with high air temperatures in the event of a fire. The paper shows the performance of fans for high operating air temperatures, up to 400 °C. The results were obtained through numerical simulations of the flow in an original design fan, whose performance was experimentally determined for normal atmospheric operating conditions ( $\rho = 1.2 \text{ kg/m}^3$ ). Performances are given for two fan speeds. Unnecessary corrections of the existing impeller design for use in jet fans for tunnel ventilation were also considered.*

Key words: *reversible fan, performance, high temperature, jet fan, efficiency, tunnel*

### Introduction

Forced air-flow (ventilation) in road tunnels can be provided by fans of different constructions. One of the methods of ventilation is using reversible jet fans [1, 2]. Reversible axial fans can provide air/gas-flows in both directions of flow, direct and opposite flow. In fans with one impeller, the flow direction is changed by changing the rotation direction of the impeller [3, 4]. These fans are used everywhere where such flow needs to be ensured, such as ventilation of tunnels, public garages, flow in brickyards, *etc.* The flow direction changes depending on the need of the technological process. When ventilating a tunnel, the flow direction is always towards low atmospheric pressure, *i.e.* in the direction of natural air-flow [2]. Often, in the event of a fire, these fans work with high air temperatures. The paper shows the performance of fans for high air temperatures: 100 °C, 200 °C, 300 °C, and 400 °C. Jet fans for tunnel ventilation should have the ability to work for a certain time with high air temperatures. The designation of such fans depends on the maximum temperature and operating time, for example, for 400 °C and two hours of operation, the designation is HT/400/2.0 [5, 6]. The aerodynamic performance of a fan for high air temperatures was obtained by numerical simulations of the flow and the application of the similarity theory in relation the performance of the fan of the original construction, whose performance was experimentally determined for normal operating conditions

\* Corresponding author, e-mail: zivan.spasic@masfak.ni.ac.rs

(air density  $\rho = 1.2 \text{ kg/m}^3$ ) [4, 7]. Jet fans for tunnel ventilation should be able to work with two rotation speeds of the impeller [1]. This paper presents the performance of a fan for the rotation speeds  $n = 1405 \text{ rpm}$  and  $2900 \text{ rpm}$ . According to the recommendations [1, 2], jet fans for tunnel ventilation should achieve an average flow velocity behind the fan of  $30\text{-}40 \text{ m/s}$ .

Longitudinal ventilation systems in tunnels with jet fans should ensure minimum air-flow velocities in the most distant parts of the tunnel but must not develop velocities that would cause damage in normal traffic. Air-flow velocities near the carriageway should be less than  $10 \text{ m/s}$  [8].

Experimental results, obtained in the laboratory in the 1:19 scale tunnel, are used for ventilation performance of the CFD test in a uni-directional traffic road tunnel [9].

For jet fans, the axial thrust generated by the fan is also important, which can be approximately determined using the expression [1, 2]:

$$F_z = \rho Qc = \rho \frac{Q^2}{A} \quad (1)$$

where  $c$  [ $\text{ms}^{-1}$ ] is the mean velocity of the current at the outlet of the fan,  $Q$  [ $\text{m}^3\text{s}^{-1}$ ] – the volume flow of the fan,  $\rho$  [ $\text{kgm}^{-3}$ ] – the air density, and  $A$  [ $\text{m}^2$ ] – the cross-sectional area of the outlet of the fan. The paper also considers the change in the thrust of the fan with the change in air temperature.

In Bogdanović-Jovanović *et al.* [10], the performance of low pressure fans operating with hot air at  $50 \text{ }^\circ\text{C}$ ,  $80 \text{ }^\circ\text{C}$ , and  $110 \text{ }^\circ\text{C}$  was considered. The change in the efficiency of the fan was observed due to the change in gas viscosity with the change in temperature. For an air temperature of  $50 \text{ }^\circ\text{C}$ , the reduction in the efficiency is less than  $0.01$  (1%), and for an air temperature of  $110 \text{ }^\circ\text{C}$ , the reduction in the efficiency is on average about  $0.02$  (2%) in relation the efficiency that the fan has at  $t = 20 \text{ }^\circ\text{C}$ .

In Abdolmaleki *et al.* [11], reversible axial flow fans, used in tunnel ventilation systems, were designed in a way that as the direction of the impeller rotation changes, suction and discharge directions change without any sensible change in flow rate and pressure. A reversible axial flow fan was studied experimentally and numerically in various ambient conditions and blade positions.

For low pressure fans, whose pressure increase in the fan is up to  $2 \text{ kPa}$  [5], the influence of the change in air density in the fan can be neglected. The change in air density due to the change in temperature cannot be neglected and significantly affects the performance of the fan. The influence of temperature change on fan performance can be determined by applying the similarity theory, observing the unchanged efficiency of the fan ( $\eta = \text{const}$ ) [12, 13].

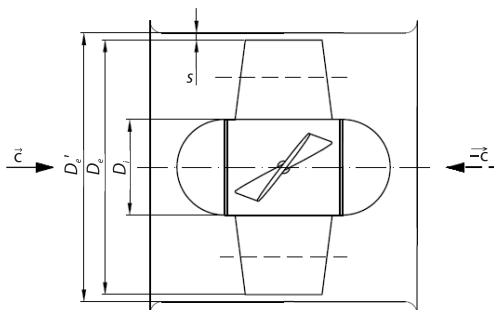


Figure 1. Geometry of the fan

### The geometry of the reversible axial fan

Reversible axial fans designed with only one impeller work reversibly, and the change in the direction of the impeller rotation changes the director of air-flow. The blades of the impeller are designed according to the model with constant specific work along the blade with symmetrical straight profiles [4, 7]. The meridian section with the dimensions of the designed axial reversible fan is shown in fig. 1. The basic dimensions of the fan are [4, 7]:

$D_e = 630$  mm is the peripheral diameter of the fan impeller,  $D_i = 300$  mm – diameter of the fan impeller hub, and  $s = 2.5$  mm is the tip clearance. The ratio of the internal and external diameter of the fan impeller is  $m = D_i / D_e = 0.48$ .

The straight profile (marked PP2) was used for the construction of the blades [7]. Straight profiles have the maximum thickness in the middle of the profile, with  $\delta_{\text{imax}} = 12$  mm at the hub and  $\delta_{\text{emax}} = 6$  mm at the shroud. The thickness distribution  $\delta_j$  along the mean line of the profile is shown in [7], with the radii of the leading and tail of the profile:  $r_x = r_{1x} = r_{2x} = 0.2 \delta_{\text{max},x}$ , fig. 2. The position of profiles in the cascade is defined by the angle of profile inclination  $\beta_i$ .

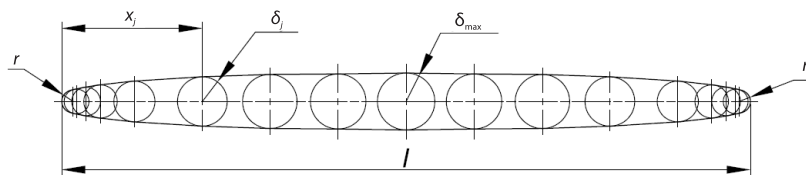


Figure 2. Symmetrical straight profile, PP2

The impeller is designed with six blades with completely symmetrical blade profiles that enable equal fan performance in direct and reversible flow. The fan is made of aluminum alloy, which is resistant to high air temperatures, fig. 3.

Experimental testing and obtaining the fan's aerodynamic characteristics were performed on a standard test installation with ducted inlet and free outlet into the atmosphere at a speed of  $n = 1405$  rpm [4, 7]. For the region of the stable performance of the fan, the diagrams of operating characteristics of the fan are shown, with total pressure rise  $\Delta p_{\text{tot}}(Q)$ , power  $P(Q)$ , and efficiency  $\eta(Q)$ , obtained for the impeller blade angle ( $\beta_L = 55^\circ$ ) and air density  $\rho = 1.2 \text{ kg/m}^3$  ( $p = 101325 \text{ Pa}$ ,  $t = 20^\circ \text{C}$ ). Using the theory of similarity [12, 13], the fan characteristics were calculated and shown for a constant rotation speed of the fan  $n = 2900$  rpm and air density  $\rho = 1.2 \text{ kg/m}^3$ , fig. 5(b).

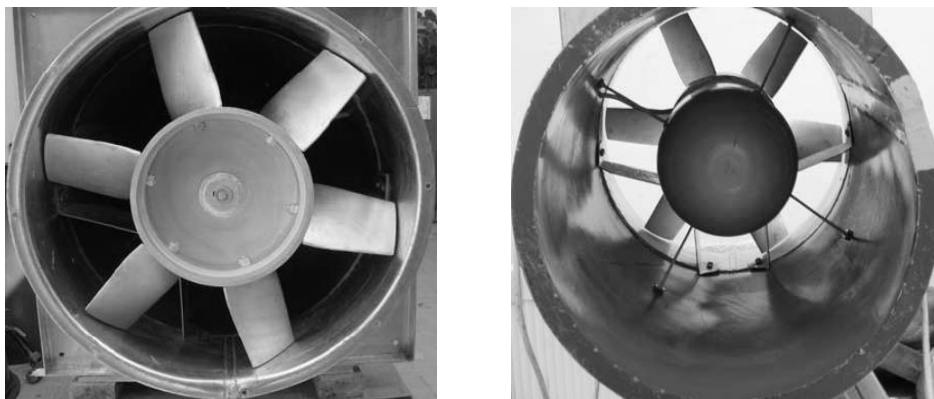


Figure 3. Reversible axial fan

The position of the blade of the impeller is defined by the angle of inclination of the blades and is equal to the angle of inclination of the skeleton chord of the blade profile at the hub of the impeller ( $\beta_L = \beta_i$ ). The model of the fan was tested for positions of impeller blade angle  $\beta_L$  measured at the hub  $\beta_L = 55^\circ$ .

### Determined performance of the fan operating with high temperatures

A change in air density due to a change in temperature can significantly affect the performance of the fan. Performance of the fan, with total pressure rise  $\Delta p_{\text{tot}}(Q)$ , power  $P(Q)$ , and efficiency  $\eta(Q)$ , operating with high temperature can be determined by numerical simulations [11, 14] or by using the theory of similarity based on the characteristics obtained for air density  $\rho = 1.2 \text{ kg/m}^3$  ( $p = 101325 \text{ Pa}$ ,  $t = 20 \text{ }^\circ\text{C}$ ).

The operating characteristics of the fan for constant rotation speeds ( $n = 1405 \text{ rpm}$  and  $n = 2900 \text{ rpm}$ ) and high air temperatures ( $100 \text{ }^\circ\text{C}$ ,  $200 \text{ }^\circ\text{C}$ ,  $300 \text{ }^\circ\text{C}$ , and  $400 \text{ }^\circ\text{C}$ ) are determined and shown here.

### Determination of fan performance on the basis of the similarity law

Aerodynamic performance of the fan for a given geometry, other rotation speed ( $n'$ ) and other atmospheric conditions, *i.e.* other air density ( $\rho'$ ), can be determined by recalculating the characteristics using the similarity theory based on the known performance for the parameter ( $n$  and  $\rho$ ). Fan performance determined on the basis of the similarity law refers to equal coefficients such as flow ( $\varphi = \varphi'$ ), pressure ( $\psi = \psi'$ ), power ( $\lambda = \lambda'$ ) and efficiency ( $\eta = \eta'$ ) [10, 12]. For changed operating conditions, volume flow, total pressure rise and power can be determined using the equations, respectively:

$$Q' = Q \frac{n'}{n}, \Delta p'_{\text{tot}} = \Delta p_{\text{tot}} \frac{\rho'}{\rho} \left( \frac{n'}{n} \right)^2, \text{ and } P' = P \frac{\rho'}{\rho} \left( \frac{n'}{n} \right)^3 \quad (2)$$

Based on the previous equations, it can be concluded that the volume flow does not change with the change in density, and that the total pressure rise and the fan power change linearly with the change in air density.

On the basis of eq. (2), the following operating characteristics of the fan can be determined: total pressure rise curve  $\Delta p'_{\text{tot}}(Q)$  and power curve  $P'(Q)$  for changed operating conditions of the fan at constant efficiency  $\eta'(Q) = \eta(Q)$ .

### Determination of fan performance based on numerical simulation

Commercial software ANSYS FLUENT (version 22) was used for numerical simulations. The geometry of the model was formed by drawing a 3D model in the part of the software for designing the impeller of turbomachines, ANSYS CFX-BladeGen, fig. 4(a). The simulated domain is defined by the boundaries of the inlet and outlet from the impeller, hub, casing and blades of the impeller, fig. 4(b). The geometry of the blades is defined through seven cylindrical sections to which the geometry of the profile is applied [7].

In this program, the user first defines the input and output of the simulated domain, which are a distance of 100 mm in front of, or behind, the impeller axis perpendicular to the axis of rotation, fig. 4(b). There are around 1200000 mesh elements for 1/6 of the fan impeller in all simulations. The mesh is formed from the topology (H/F/C/L-grid) with a mesh around the profile (O-grid). Its settings are adjusted in line with the criteria recommended for maximum and minimum values of the elements: the relation between the edges, volume ratio and angle elements [7].

Rotating motion of the impeller is defined as the axis of rotation and rotational speed ( $n = 1405 \text{ rpm}$  and  $n = 2900 \text{ rpm}$ ). Each interface geometry gets its boundary conditions (input, output, solid surfaces-walls) and the initial value of the total pressure at the entrance

( $p_{\text{tot}} = 100 \text{ kPa}$ ) and the desired mass fan flow. In the case of a multi-domain model, the places in which these domains merge (interfaces) need to be defined. The simulation is performed only in the space surrounding one blade, because of the impeller symmetry, thus it is necessary to define the periodic surfaces of the flow field as well. The program can define the type of fluid and its physical properties, the turbulence model (here, the  $k-\varepsilon$  model), and the criteria for numerical calculations (convergence – residual  $10^{-5}$ , the maximum number of iterations, the level of resolution, *etc.*)

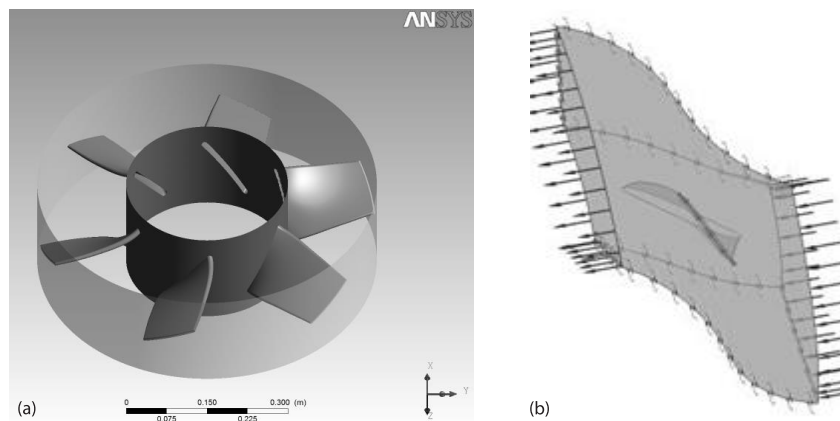


Figure 4. (a) fan model for simulation and (b) simulated domain

Numerical determination of operating characteristics was performed on a fan model with straight blade profiles for positions of impeller blade angle measured at the hub  $\beta_L = 55^\circ$ . The simulations were performed for the rotation speeds  $n = 1405 \text{ rpm}$  and  $2900 \text{ rpm}$ . Simulations were performed for normal atmospheric operating conditions ( $\rho = 1.2 \text{ kg/m}^3$ ) and for high air temperatures:  $100^\circ\text{C}$ ,  $200^\circ\text{C}$ ,  $300^\circ\text{C}$ , and  $400^\circ\text{C}$ . The results of numerical simulations are presented in graphs  $\Delta p(Q)$ ,  $\eta(Q)$ , and  $P(Q)$ , which are given on the basis of the averaged values of simulation for the middle cylindrical section of the impeller, for different air temperatures. The results are shown by dashed lines in figs. 5-7.

#### **Performance of the fan using the theory of similarity and numerical simulations**

For the region of the stable performance of the fan, the diagrams of operating characteristics show total pressure rise  $\Delta p_{\text{tot}}(Q)$ , fig. 5, power  $P(Q)$ , fig. 6, and efficiency  $\eta(Q)$ , fig. 7, obtained for a constant rotation speed of the fan for  $n = 1405 \text{ rpm}$  and  $n = 2900 \text{ rpm}$  for air density  $\rho = 1.2 \text{ kg/m}^3$  and for high air temperatures:  $100^\circ\text{C}$ ,  $200^\circ\text{C}$ ,  $300^\circ\text{C}$ , and  $400^\circ\text{C}$ .

The diagrams, (figs. 5-7) show the operating characteristics obtained experimentally for air density  $\rho = 1.2 \text{ kg/m}^3$  ( $p = 101325 \text{ Pa}$ ,  $t = 20^\circ\text{C}$ ), on the basis of the numerical simulations (dashed lines, labelled num) and on the basis of the similarity law (solid lines, labelled sim) for high air temperatures.

Analysis of the results, fig. 5: for the air temperature  $t = 20^\circ\text{C}$ , numerical simulations yielded higher pressure rise values than the values obtained by the experiment, and for the entire domain of the tested flow this difference is greater for a higher rotation speed. As the flow rate increases, this difference decreases. With the increase in air temperature (decrease in air density), the pressure increase curves yielded by numerical simulations and the similarity law become closer, so that at high temperatures ( $200\text{-}400^\circ\text{C}$ ) they almost overlap for the rotation speed  $n =$

2900 rpm, while for the number  $n = 1405$  rpm they overlap at  $100\text{ }^{\circ}\text{C}$ , and for higher temperatures the curves yielded by numerical simulations are below the curves yielded by the similarity law.

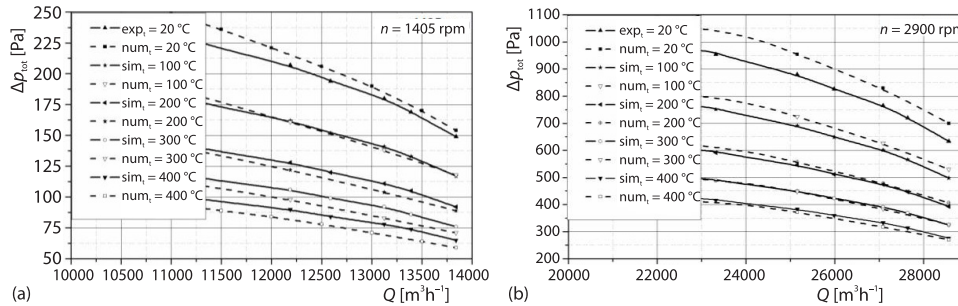


Figure 5. Total pressure rise of the fan,  $\Delta p_{tot}(Q)$ ; (a)  $n = 1405$  rpm and (b)  $n = 2900$  rpm

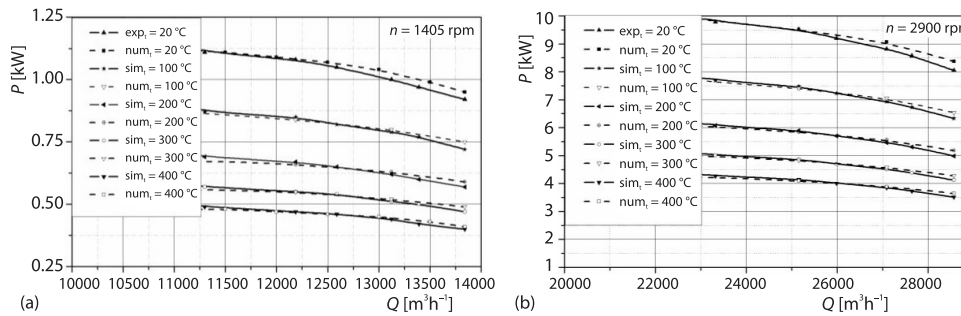


Figure 6. Power characteristics,  $P(Q)$ ; (a)  $n = 1405$  rpm and (b)  $n = 2900$  rpm

Analysis of the results, fig. 6: the power curves yielded by numerical simulations generally coincide with the curves yielded by the similarity law for both speeds and all temperature values. For higher flows, the curves are more separated.

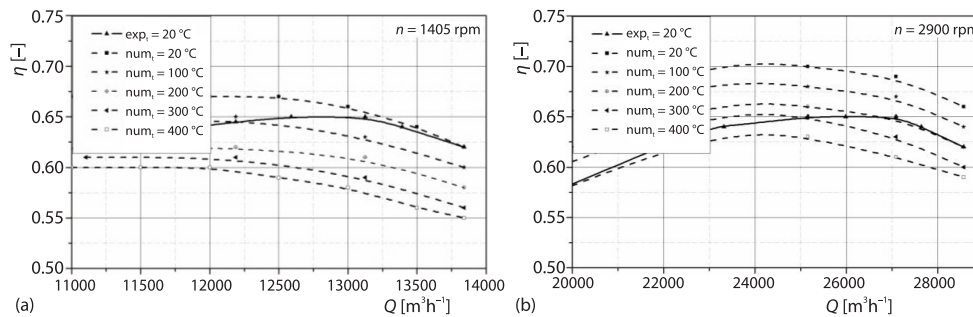


Figure 7. Efficiency characteristics,  $\eta(Q)$ ; (a)  $n = 1405$  rpm and (b)  $n = 2900$  rpm

Analysis of the results, fig. 7: numerical simulations show a decrease in efficiency by about 0.04 (4%) for every temperature increase of  $100\text{ }^{\circ}\text{C}$ . The efficiency curves for the rotation speed  $n = 1405$  rpm and  $t = 20\text{ }^{\circ}\text{C}$  are calculated for flows greater than  $13300\text{ m}^3/\text{h}$ , while the simulations for higher temperatures yielded lower efficiency values.

For the rotation speed  $n = 2900$  rpm and  $t = 20\text{ }^{\circ}\text{C}$ , fig. 7(b) the efficiency values yielded by numerical simulations are higher than the values yielded by the experiment by about 0.08 (8%). For each temperature increase of  $100\text{ }^{\circ}\text{C}$ , numerical simulations yielded efficiency

values lower by about 0.04 (4%). The maximum values of efficiency (optimal working point of the fan) yielded by numerical simulations move to the left (toward lower flows) with increasing temperature.

The higher values of pressure rise and efficiency yielded by numerical simulations are explained by the fact that the simulations did not cover the entire domain where the experiment was performed, where hydraulic losses are higher. Numerical simulations did not take into account the influence of the flow of the cylindrical part with a spherical face, which ensures an even flow of air on the blades of the impeller. Numerical simulations actually yield the internal efficiency of the fan, which does not take into account the friction of the air on the surfaces of the hub with the ends of the screws and nuts for attaching the blades to the hub.

*Correction of the efficiency of the fan due to the reduction of the Reynolds number*

To establish a dynamic similarity with fans, the condition of equality of the Reynolds number ( $Re = Re'$ ) should be met, where the  $Re'$  number is for air-flow regime with high air temperatures. The Reynolds number is defined [10, 12]:

$$Re = \frac{uD}{\nu} = \frac{\pi n D^2}{\nu} \quad (3)$$

For normal fan operating conditions ( $p = 101325 \text{ Pa}$ ,  $t = 20 \text{ }^\circ\text{C}$ ) air characteristics are: air density  $\rho = 1.2 \text{ kg/m}^3$ , kinematic viscosity  $\nu = 1.530 \cdot 10^{-5} \text{ m}^2/\text{s}$  and  $Re = 6.25 \cdot 10^6$ .

As the air temperature increases, the air density decreases, the kinematic viscosity increases and the Reynolds number decreases, eq. (2). Data for high air temperatures and pressure  $p = 1 \text{ bar}$  are shown in tab. 1.

**Table 1. Data for high air temperatures and pressure  $p = 1 \text{ bar}$  [15]**

Air temperatures [ $^\circ\text{C}$ ]	Density, $\rho$ [ $\text{kgm}^{-3}$ ]	Kinematic viscosity, $\nu$ [ $\text{m}^2\text{s}^{-1}$ ]	Reynolds number [-]
100	0.934	$2.315 \cdot 10^{-5}$	$4.13 \cdot 10^6$
200	0.737	$3.494 \cdot 10^{-5}$	$2.74 \cdot 10^6$
300	0.608	$4.809 \cdot 10^{-5}$	$1.99 \cdot 10^6$
400	0.518	$6.295 \cdot 10^{-5}$	$1.52 \cdot 10^6$

Due to the unfulfilled condition of dynamic similarity of flow in axial fans, efficiency  $\eta'$  can be approximately calculated using the empirical Stephenson formula [10, 12]:

$$\eta' = \eta + \frac{1558}{Re'^{0.2}} \left[ \left( \frac{Re'}{Re} \right)^{0.2} - 1 \right] \quad (4)$$

which is valid for  $Re > 0.5 \cdot 10^5$ . For the optimal operating regime of the fan ( $\eta = \eta_{\text{max}}$ ), the correction of the efficiency can be performed using the Ackert formula [10, 12]:

$$\eta' = 1 - \frac{1 - \eta}{2} \left[ 1 + \left( \frac{Re'}{Re} \right)^{0.2} \right] \quad (5)$$

Figure 8 shows the corrected efficiency curves (solid lines, labelled corr) obtained by

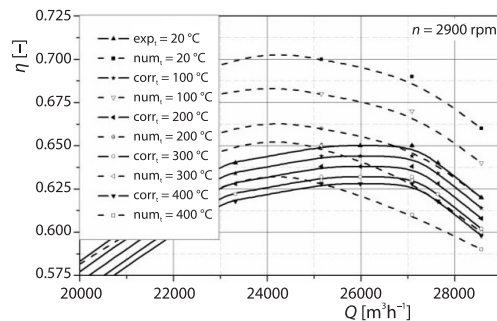


**Figure 8. Change in efficiency characteristics with change in air temperature**

using eq. (4) due to the decrease in the Reynolds number due to the increase in air temperature. It can be seen from the figure that the decrease in efficiency is negligible, for every 100 °C increase in temperature, the decrease in efficiency is slightly less than 0.01 (less than 1%).

Using eq. (5) for efficiency correction also results in a small decrease in efficiency for the optimal operating mode of the fan, about 0.01 (1%) for every 100 °C increase in air temperature. Those values are not shown in the paper.

Similar values of efficiency reduction due to temperature increase were also obtained for the rotation speed  $n = 1405$  rpm.

### Possibility of operation of the reversible axial fan as a jet fan

A reversible axial fan, used as a jet fan for tunnel ventilation, should have the ability to work with two rotation speeds. When the fan works with high air temperatures (in the case of a fire) it works with a higher rotation speed, in this case  $n = 2900$  rpm.

For the operation of a reversible axial fan as a jet fan, the maximum flow with a minimum increase in pressure is important, because a jet fan is used for producing a jet of air in a space and is unconnected to any ducting. From the diagram, fig. 5(b), it can be seen that the fan achieves a maximum flow of  $Q = 28600 \text{ m}^3/\text{h} = 7.94 \text{ m}^3/\text{s}$  (for  $n = 2900$  rpm). At that flow, the air-flow velocity at the outlet of the fan is:

$$c_z = \frac{4Q}{D_e^2 \pi} = \frac{4 \cdot 7.94}{0.63^2 \pi} = 25.5 \text{ m/s} \quad (6)$$

The total pressure rise in the fan is equal to the sum of static,  $p$ , and dynamic pressure:

$$\Delta p_{\text{tot}} = p + \rho \frac{c^2}{2} \quad (7)$$

If the fan were to work as a jet fan, in a free stream of air ( $p = 0$ ), that is without suction and pressure pipes, then the theoretical velocity of air-flow at the outlet of the fan can be determined from the total pressure rise of the fan. For the operating point with maximum flow, fig. 5(b), the total pressure rise is  $\Delta p_{\text{tot}} = 630$  Pa, and the theoretical velocity of air-flow can be determined based on the equation:

$$c_{zt} = \sqrt{\frac{2\Delta p_{\text{tot}}}{\rho}} = \sqrt{\frac{2 \cdot 630}{1.2}} = 32.4 \text{ m/s} \quad (8)$$

For air temperature  $t = 400$  °C ( $\rho = 0.518 \text{ kg/m}^3$ ) and total pressure rise  $\Delta p_{\text{tot}} = 260$  Pa, the theoretical velocity is  $c_{zt} = 31.6$  m/s. What could be concluded is that such a fan with a rotation speed  $n = 2900$  rpm could work as a jet fan with the power of the driving electric motor of around 8 kW.

An increase in the flow of the axial fan, for the same rotation speed, can be achieved by turning the blades of the impeller or by increasing the number of blades, but in doing so, the increase in power should be taken into account. Increasing the air speed at the outlet of the fan can also be achieved by reducing the cross-sectional area of the outlet of the fan by installing a cylindrical cone that will direct the air. In this way, the increase in air-flow velocity is achieved without increasing the power.

Based on eq. (1), the thrust amounts to ( $\rho = 1.2 \text{ kg/m}^3$ ):

$$F_z = 1.2 \frac{4 \times 7.94^2}{0.63^2 \pi} = 242.8 \text{ Nm} \quad (9)$$

With an increase in temperature, the volume flow does not change, and therefore, the velocity of the air-flow at the outlet of the fan does not change, but the thrust changes due to the change in air density, eq. (1):

$$F'_z = \frac{\rho}{\rho'} F_z \quad (10)$$

With increased air temperature, the air density decreases, and with that, the thrust decreases proportionally, which should be taken into account when designing the fan.

In order for the axial reversible fan to work as a jet fan, all characteristics should be determined in accordance with the ISO 13350 standard [16]. The reversible fan has a tip clearance of 2.5 mm, however, due to the possible operation of the fan at high temperatures, dilatation of the elements may occur, so the size of the tip clearance should be increased.

### Conclusions

In the case of low pressure fans whose pressure increase in the fan is less than 2 kPa, the influence of the change in air density due to the change in pressure in the fan can be ignored, but the change in air density due to the change in temperature cannot be ignored and can significantly affect the performance of the fan.

Based on the obtained fan characteristics  $\Delta p_{\text{tot}}(Q)$  and  $P(Q)$ , figs. 5. and 6, from numerical simulations and by recalculating the characteristics using the similarity law, approximately the same values are obtained for high air temperatures, so both methods can be used in practice. The decrease in fan efficiency with the increase in air temperature is small, so it can be ignored.

With an increase in air temperature, the volume flow of the fan does not change, but the air density does. With an increased air temperature, the air density decreases and therefore, the thrust decreases proportionally, which should be taken into account when designing the fan.

The average velocity of the flow at the outlet of the jet fan should be greater than 30 m/s, this can be achieved by increasing the flow rate. At a constant rotation speed, the flow of axial fans can be increased by turning the blades of the impeller, *i.e.* by increasing the angle of inclination of the blades. Increasing the air speed at the outlet of the fan can also be achieved by reducing the outlet cross-section of the fan by installing a cylindrical cone that would direct the air.

Due to the possible operation of the fan at high temperatures, dilatation of the elements may occur, so it is necessary to take into account the construction of the fan itself, and especially the size of the tip clearance.

The size of the maximum flow of the fan, obtained experimentally on the installation with ducted inlet and free outlet into the atmosphere, will certainly achieve a higher flow if the fan works in a free stream of air, as the jet fan does.

The mentioned construction of the axial reversible fan with the rotation speed  $n = 2900$  rpm can work as a jet fan for ventilating tunnels if the mentioned corrections are made and the given recommendations are taken into account. It is necessary to examine the acoustic characteristics of the given fan, which were not considered here.

### Acknowledgment

This research was financially supported by the Ministry of Science, Technological Development and Innovation of the Republic of Serbia (Contract No. 451-03-47/2023-01/200109).

## Nomenclature

$c$  – velocity, [ms<sup>-1</sup>]  
 $D$  – diameter, [m]  
 $F_z$  – thrust, [N]  
 $l$  – profile length, [m]  
 $n$  – rotation speed, [rpm]  
 $P$  – power, [W]  
 $\Delta p_{\text{tot}}$  – total pressure rise, [Pa]  
 $Q$  – flow, [m<sup>3</sup>s<sup>-1</sup>]  
 $s$  – tip clearance, [m]  
 $u$  – impeller tip speed velocity, [ms<sup>-1</sup>]

## Greek letters

$\beta_l$  – impeller blade angle [°]  
 $\delta$  – thickness profile, [m]  
 $\eta$  – efficiency, [-]

## Subscripts

e – periphery  
 i – for hub  
 t – mean line, theoretical

## References

- [1] Benišek, M. H., *et al.*, New Design of the Reversible Jet Fan, *Processes*, 8 (2020), 12, pp. 1671-1683
- [2] Tarada, F., Brandt, R., Impulse Ventilation for Tunnels – A State of the Art Review, *Proceedings*, 13<sup>th</sup> International Symposium on Aerodynamics and Ventilation of Vehicle Tunnels, New Brunswick, N. J., USA, 2009, Vol. 3, pp. 1067-1070
- [3] Krsmanović, L. J., Gajić, A., *Turbomachinery – Fans*, (in Serbian), Faculty of Mechanical Engineering, University of Belgrade, Belgrade, Serbia, 2000
- [4] Spasić, Ž., Numerical and Experimental Investigation of the Influence of the Blade Profile Shape on the Reversible Axial Fan Characteristics (in Serbian), Ph. D. thesis, Faculty of Mechanical Engineering Nis, University of Nis, Nis, Serbia, 2012
- [5] \*\*\*, ISO 13349:2010 Fans for general purposes – Vocabulary and definition of categories; ISO: Geneva, Switzerland, 2010
- [6] \*\*\*, EN 12101-3:2015 Smoke and heat control systems – Part 3: Specification for powered smoke and heat control ventilators (Fans), European Committee for Standardization, Brussels, Belgium, 2015
- [7] Spasić, Ž., *et al.*, Low-pressure Reversible Axial Fan with Straight Profile Blades and Relatively High Efficiency, *Thermal Science*, 16 (2012), Suppl. 2 pp. S605-S616
- [8] Stašević, M. M., *et al.*, Some Aspects of Design Ventilation System in Road Tunnels, *Thermal Science*, 26 (2022) 4B, pp. 3587-3596
- [9] Šekularac, M. B., Janković, N. Z., Experimental and numerical Analysis of Flow Field and Ventilation Performance in a Traffic Tunnel Ventilated by Axial Fans, *Theor. Appl. Mech.*, 45 (2018), 2, pp. 151-165
- [10] Bogdanović-Jovanović, J. B., *et al.*, Performance of Low-Pressure Fans Operating with Hot Air, *Thermal Science*, 20 (2016), Suppl. 5, pp. S1435-S1447
- [11] Abdolmaleki, M., *et al.*, Numerical and Experimental Study of a Reversible Axial Flow Fan, *International Journal of Computational Fluid Dynamics*, 34 (2020), 3, pp. 173-186
- [12] Rangwala, A. S., *Turbo-Machinery Dynamics, Design and Operation*, McGraw-Hill, New York, USA, 2005
- [13] Bogdanović, B., *et al.*, *Fans-Performance and Operating Characteristics* (in Serbian), Faculty of Mechanical Engineering Nis, Nis, Serbia, 2012
- [14] Spasić, Ž., *et al.*, Numerical Investigation of the Influence of the doubly Curved Blade Profiles on the Reversible Axial Fan Characteristics, *Facta Universitatis, Series: Mechanical Engineering*, 18 (2020), 1, pp. 57-68
- [15] Djordjević, B., *et al.*, *Thermodynamics with Thermotechnics* (in Serbian), Faculty of Technology and Metallurgy, Belgrade, Serbia, 2003
- [16] \*\*\*, ISO 13350:2015, Fans-Performance Testing of Jet Fans; ISO: Geneva, Switzerland, 2015